

Avalanche multiplication phenomenon in amorphous semiconductors: Amorphous selenium versus hydrogenated amorphous silicon

A. Reznik^{a)}

Imaging Research, Sunnybrook Health Sciences Centre, Toronto, M4N 3M5, Canada

S. D. Baranovskii and O. Rubel

Department of Physics and Material Sciences Center, Philipps University Marburg, D-35032 Marburg, Germany

G. Juska

Faculty of Physics, Vilnius University, Sauletekio 9, Vilnius, 10222, Lithuania

S. O. Kasap

Department of Electrical Engineering, University of Saskatchewan, 57 Campus Drive, Saskatoon, SK, S7N 5A9, Canada

Y. Ohkawa and K. Tanioka

NHK Science and Technical Research Laboratories, 1-10-11 Kinuta, Satagaya-Ku, Tokyo, 157-8510, Japan

J. A. Rowlands

Toronto Sunnybrook Regional Cancer Centre, Toronto, M4N 3M5, Canada

(Received 26 March 2007; accepted 17 July 2007; published online 14 September 2007)

Although the effect of the impact ionization and the consequent avalanche multiplication in amorphous selenium (*a*-Se) was established long ago and has led to the development and commercialization of ultrasensitive video tubes, the underlying physics of these phenomena in amorphous semiconductors has not yet been fully understood. In particular, it is puzzling why this effect has been evidenced at practical electric fields only in *a*-Se among all amorphous materials. For instance, impact ionization seems much more feasible in hydrogenated amorphous silicon (*a*-Si:H) since the charge carrier mobility in *a*-Si:H is much higher than that in *a*-Se and also the amount of energy needed for ionization of secondary carriers in *a*-Si:H is lower than that in *a*-Se. Using the description of the avalanche effect based on the lucky-drift model recently developed for amorphous semiconductors we show how this intriguing question can be answered. It is the higher phonon energy in *a*-Si:H than that in *a*-Se, which is responsible for the shift of the avalanche threshold in *a*-Si:H to essentially higher fields as compared to *a*-Se. © 2007 American Institute of Physics. [DOI: 10.1063/1.2776223]

I. INTRODUCTION

Impact ionization leading to avalanche multiplication was discovered and explained in amorphous selenium (*a*-Se) in 1980.¹ While this discovery was initially greeted with skepticism over the years, avalanche multiplication has been not only confirmed by numerous experiments, but has been also utilized in commercial *a*-Se photoconductive targets used in ultrasensitive high-gain avalanche rushing photoconductor (HARP) TV camera tubes and complementary metal-oxide-semiconductor (CMOS) imagers.²⁻⁴ It has been proposed that, due to their ultrahigh sensitivity, provided by avalanche gain *a*-Se, HARP photosensors will be a promising approach for low-dose x-ray imaging detectors and a viable alternative to photomultiplier tubes for functional medical imaging (i.e., positron emission tomography).⁵⁻⁷ Even though the experimental evidence for avalanche multiplication in *a*-Se is clear cut, the theoretical understanding of the origin and nature of this phenomenon in amorphous semiconductors has remained unresolved. The mean-free

paths in these semiconductors are so short (compared to the typical mean-free path in crystalline materials) that impact ionization has been difficult to understand. Recently, it has been possible to formulate an explanation for the avalanche multiplication mechanism in *a*-Se in terms of the modified lucky-drift (LD) model,⁸ which had been originally proposed for crystalline semiconductors by Ridley,^{9,10} Burt,¹¹ and Mackenzie and Burt^{12,13} in the 1980s. The main difference between the lucky drift model and the conventional (Shockley) model, is that the lucky drift allows carriers to scatter between impact ionization events. This results in a higher probability for buildup of sufficient energy (by drifting in the electric field) to initiate impact ionization. For *a*-Se it was shown⁸ that the LD model predicts the experimental impact ionization coefficient (IIC) versus field data. Furthermore, the LD model shows that impact ionization occurs preferentially across the entire band gap rather than from midgap to the extended states close to the band edge.¹⁴

Although the LD model clarifies the origin of avalanche multiplication in amorphous media, it is still unclear why *a*-Se shows avalanche multiplication much more clearly than other amorphous materials, even for those with much nar-

^{a)}Electronic mail: alla.reznik@sunnybrook.ca

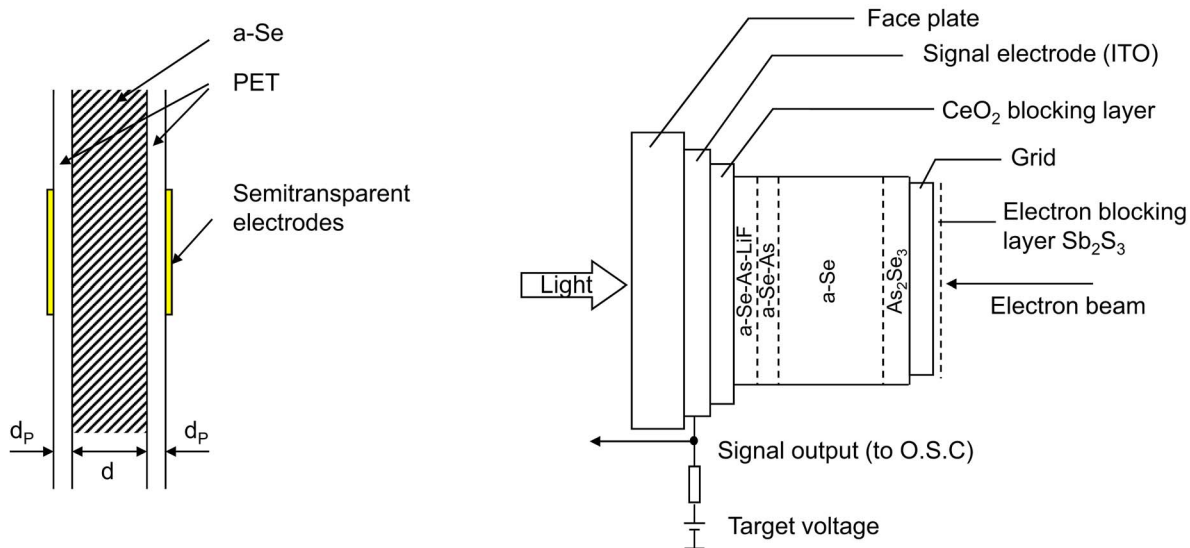


FIG. 1. Schematic picture of *a*-Se structures under investigation here: (a) insulating structure; (b) blocking HARP structures.

rower band gaps. Indeed, to the best of our knowledge, there is no unequivocal experimental evidence for avalanche multiplication in any other amorphous material, although there is some evidence for the first stage of avalanche multiplication (impact ionization) in some chalcogenide glasses. In some glasses based on Te, As, Ge, and Si,¹⁵ impact ionization is a possible explanation for the threshold switching behavior seen in these materials.¹⁶ As for the most studied amorphous semiconductor material, *a*-Si:H, most attempts to reach avalanche multiplication have been futile.^{17–19} For example, Futaka *et al.*¹⁸ prepared vidicon-type *n-i-p* *a*-Si:H devices, applied fields as high as $80 \text{ V}/\mu\text{m}$, and observed no avalanche multiplication. However, at much higher fields ($\sim 150 \text{ V}/\mu\text{m}$) Akiyama *et al.*²⁰ explain their results on photocurrent in a double-heterostructure-type device (*p*-type *a*-Si:H, *i*-type *a*-Si:H deposited onto an *n*-type crystalline substrate) in terms of avalanche multiplication. Since the ionization energy of impact ionization (i.e., the threshold energy for ionization) for many semiconductors, typically, decreases with the band-gap energy,²¹ it is quite surprising that while *a*-Se with $E_g \geq 2.0 \text{ eV}$ exhibits clear avalanche multiplication, the onset of impact ionization in *a*-Si:H with $E_g \approx 1.7\text{--}1.8 \text{ eV}$ occurs only at much higher fields.

We have investigated avalanche multiplication in two different *a*-Se structures and have measured the dependence of the effective quantum efficiency (η^*) on electric field F . Thicker samples show a higher avalanche gain, which is a distinct advantage in practical applications. From the experiments, we have determined IIC dependence on F and compared it with the theoretical dependence calculated in terms of the lucky-drift model.⁸ This identified the carrier scattering parameters in *a*-Se. It is proposed that the different avalanche behavior of *a*-Si:H compared to *a*-Se is due to much higher phonon energies in *a*-Si:H that might arise from phonon local modes associated with hydrogen.

II. EXPERIMENTAL DETAILS

A. Effective quantum efficiency in *a*-Se

Traditionally, the term quantum efficiency (η) has been used to describe the dissociation efficiency of electron–hole pairs (EHPs) after photon absorption. Here, we introduce effective quantum efficiency η^* that is a modified definition of quantum efficiency: η^* incorporated both the primary mechanism by which EHPs are generated and also the secondary mechanism by which these freed carriers can multiply, i.e., avalanche. This is the quantity of highest practical importance and is the directly measured quantity in F -dependent measurements of photocurrent.

For blue light, η^* and IIC were investigated for two types of *a*-Se structures, namely, (1) an insulating structure and (2) a HARP blocking structure.

For the insulating structure, *a*-Se layers (thickness $d = 4\text{--}33 \mu\text{m}$) were sandwiched between two insulating polyethyleneterephthalat (PET) layers with semitransparent metal electrodes deposited on the outer surfaces of the PET [Fig. 1(a)]. Use of PET layers prevents carrier injection from the electrodes and permits high-voltage biasing during photocurrent measurements without excessive dark current.^{1,22} F has been calculated from the total applied voltage and known capacitance of all layers. η^* was derived by time integrating the *a*-Se transient photocurrent produced by single-pulse (1 ns) illumination. By illuminating either the anode or the cathode surfaces, the photogeneration and transport of either holes or electrons, respectively, were studied. After each measurement the charge trapped at the *a*-Se/PET interface was eliminated and the sample reset to its initial state by shorting the electrodes and resting the sample for 5 min. The details of the η^* measurement method can be found in Ref. 1.

In contrast, in the HARP blocking structure, there is no need for a reset stage since blocking contacts permit the exit of mobile carriers from the bulk of the photoconductor to the electrode while simultaneously preventing the injection of

carriers of opposite sign from the electrode into the photoconductor. In our samples an *a*-Se layer ($d=8\text{--}35\ \mu\text{m}$) is confined between CeO_2 and Sb_2S_3 layers, which act as blocking layers. The absence of carrier injection is confirmed by the low dark current, which does not exceed $1\ \text{nA}/\text{mm}^2$ at any F ($1\text{--}100\ \text{V}/\mu\text{m}$). The *a*-Se blocking structure used is called HARP and was developed for broadcast TV image tubes [Fig. 1(b)]. The details of the η^* measurement method have been described previously.²³

The *a*-Se HARP structure is deposited on a glass plate with an indium-tin-oxide (ITO) layer that serves as a transparent positive electrode. The back of the *a*-Se HARP structure is *free*, i.e., it has no physical electrode so that it can form a latent charge image. A scanning electron beam serves as a virtual cathode biasing the free surface [see Fig. 1(b)]. Optical photons incident on the front *a*-Se surface through the transparent, positively biased ITO electrode are absorbed and create EHPs. The free electrons are drawn the small distance to the positive electrode and captured, and so they do not contribute significantly to the photocurrent. In contrast, the freed holes drift the full thickness of the *a*-Se layer to the free surface, and thus constitute the major component of the photocurrent. At the free surface the holes accumulate as a latent charge image in an amount proportional to the incident light intensity. An electron beam scans the free surface, completing the circuit, and enables the accumulated positive charge to be sensed by the ITO electrode as a current. Thus, the use of an electron beam permits the continuous flow of current inside the *a*-Se layer, eliminating the need for resetting the structure. In theory, illumination from either side of the *a*-Se would permit the study of the transport of either electrons or holes. However, the video tube structure [Fig. 1(b)] used here permits illumination only of the positive electrode, and therefore, the study of photogeneration and transport of only holes. All experiments on the HARP blocking structure were performed using low enough light intensity to ensure small signal conditions. This prevents the buildup of space charge so that the electric field in the sample is not disrupted (that is, the photocurrent is not space-charge perturbed), and hence, a linear photoresponse is kept.

All samples show similar F dependences of η^* (Fig. 2). At $F\sim 40\ \text{V}/\mu\text{m}$, η^* saturates at unity. The threshold of avalanche multiplication is characterized by a sharp increase in η^* above unity. This threshold is thickness dependent: while for comparatively thin ($d<30\ \mu\text{m}$) films it begins at $F_{\text{th}}\sim 80\ \text{V}/\mu\text{m}$, for thicker films the onset occurs at slightly lower F_{th} ($\sim 70\ \text{V}/\mu\text{m}$).¹ Since only holes undergo multiplication, η^* depends on the *a*-Se layer thickness d as

$$\eta^* = \exp(\alpha \times d), \quad (1)$$

where α is the hole IIC. Thus, we can calculate the field dependence of α using the experimentally determined dependence of η^* on F . Thus obtained, α is plotted versus $1/F$ in Fig. 3. A rapid increase in α with F is seen at high F (hole avalanche regime) for both insulating and blocking structures.

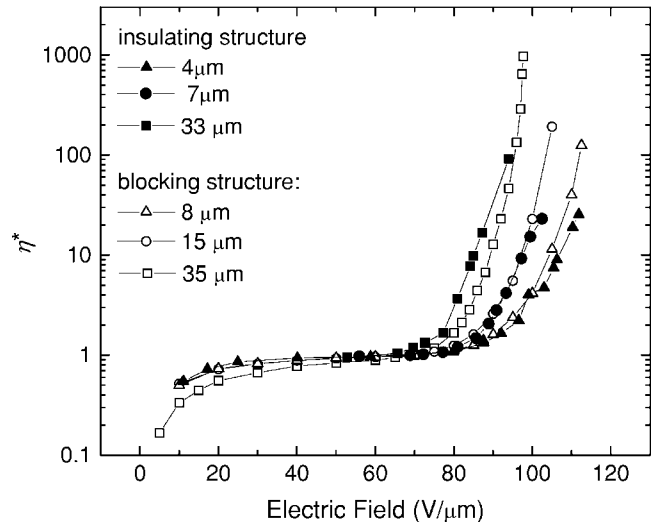


FIG. 2. Field dependence of the effective quantum efficiency for both the insulating *a*-Se structure and blocking *a*-Se HARP structure for various thicknesses.

B. Effective quantum efficiency in *a*-Si:H

Two types of *a*-Si:H structures were measured at F up to $50\ \text{V}/\mu\text{m}$, (1) blocking structure, *a*-Si:H *p-i-n* ($d=5\text{--}50\ \mu\text{m}$), and (2) insulating structure consisting of a $d=18\ \mu\text{m}$ intrinsic *a*-Si:H film between insulating layers.²⁴ Neither structure showed charge multiplication for any combination of d or F . This conclusion was confirmed by Chevrier *et al.*¹⁹ for $d=10\ \mu\text{m}$ *a*-Si:H *p-i-n* structures for $F<100\ \text{V}/\mu\text{m}$. There is, however, suggestion for *a*-Si:H avalanche multiplication in considerably higher fields ($F\geq 150\ \text{V}/\mu\text{m}$).²⁰ Figure 4 shows the data of Akiyama *et al.*²⁰ for η^* as a function of F . The lines $\eta^*=1.5$ and 2 highlight the large field required for impact ionization in *a*-Si:H ($\sim 170\ \text{V}/\mu\text{m}$ and $\sim 200\ \text{V}/\mu\text{m}$, respectively).

III. LUCKY-DRIFT MODEL OF AVALANCHE MULTIPLICATION

In order to describe the avalanche multiplication phenomenon in *a*-Se theoretically, we will use the so-called

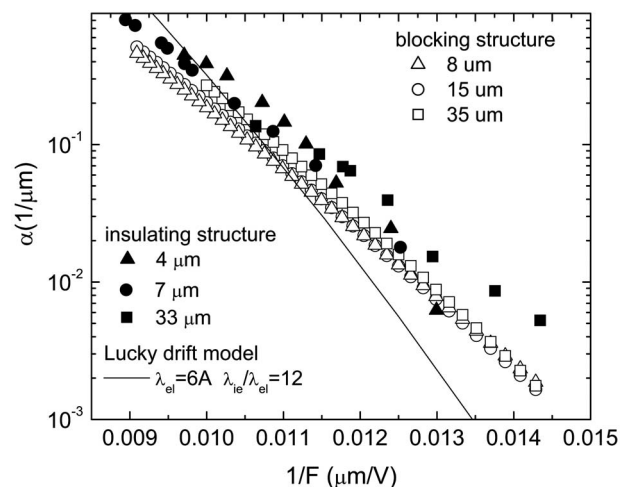


FIG. 3. Experimentally determined IIC (symbols) plotted vs. reciprocal electric field for different *a*-Se samples (both insulating and HARP blocking structures) and calculated IIC (line). Material parameters for the calculations are: $E_c=2.3\ \text{eV}$, $E_r=31\ \text{meV}$, $\lambda_{ei}=6\ \text{\AA}$, and $\lambda_{ie}/\lambda_{ei}=12$.

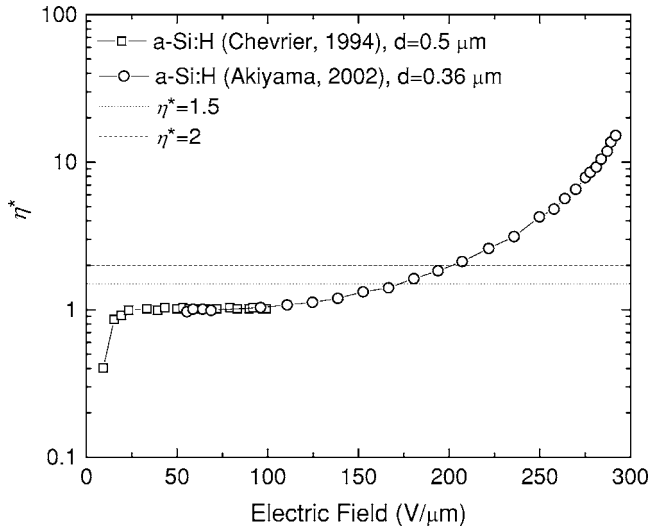


FIG. 4. Effective quantum efficiency vs. electric field for a -Si:H ($E_g = 1.8$ eV) from two different published works: Chevrier and Akiyama as discussed in the text.

lucky-drift model. This model has been suggested by Ridley⁹ and later developed by McKenzie and Burt¹³ for description of impact ionization in crystalline semiconductors. This model has been used to account for the avalanche phenomenon also in a -Se.¹⁴ One of the key features of this LD model is the assumption that primary charge carriers undergo either elastic scattering collisions, which lead to the momentum relaxation, or inelastic collisions, in which they lose their kinetic energy completely. Herewith the processes in which charge carriers lose just some fraction of their kinetic energy were neglected.^{9,13,14} It seems, however, not probable that carriers either do not lose energy at all or lose their total energy in a single scattering event. In order to overcome this deficiency of the LD model in its initial formulation, Rubel *et al.*⁸ have modified the LD model by taking into account also scattering processes that lead to the loss of a *fraction* of the kinetic energy of charge carriers. The example of the latter processes is the scattering on optical phonons. In this paper we use this modified version of the LD model, which we only briefly describe below. A detailed description of this modified LD model can be found in Ref. 8.

It is assumed⁸ that primary charge carriers undergo two kinds of scattering events while drifting under F : elastic scattering on disorder potential fluctuations and inelastic collisions with phonons. The elastic scattering process is characterized by the mean-free path λ_{el} , which is of the order of an interatomic spacing. The scatterers are distributed randomly in space, and the angle θ with respect to the field after each collision event is treated as random. (There is always some velocity component along F after an elastic scattering process.) Inelastic scattering is characterized by the mean-free path λ_{ie} . We will assume that the energy loss of a primary charge carrier in each inelastic collision with phonons is of the order of the optical phonon energy E_r .

A primary charge carrier can gain the energy E_c necessary for ionization of the secondary EHP from the F in a series of lucky collision events. Since for amorphous materials ionizing excitation across the mobility gap is much

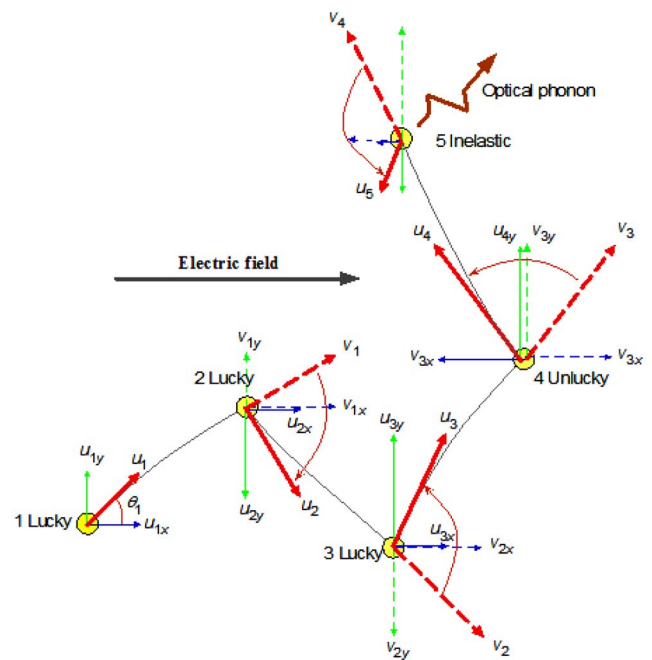


FIG. 5. Highly simplified schematic illustration of lucky drift in a field along the x direction in terms of four elastic (three lucky and one unlucky) collisions that yield a drift velocity along the field and allow the kinetic energy to be built up. Collision 5 is inelastic and the hole loses an optical phonon energy. Right after collision 1, a hole starts with an initial velocity u_1 with components u_{1x} and u_{1y} along x and y . u_{1x} builds up while u_{1y} remains the same until the next elastic collision 2. Just before the collision, the “final” velocities are v_1 , $v_{1x} = u_{1x} + a\tau$ (a -acceleration, τ -mean-free time). The elastic collision ensures that the initial velocity u_2 after collision 2 is the same as the final velocity v_1 before the collision. The y -component velocity direction (whether it is positive or negative) is *random* after the collision. While the average velocity along the field does not build up, there is a buildup in the kinetic energy because the overall velocity builds up from v_1 to v_2 to v_3 but v_4 is smaller than v_3 due to the fourth collision being unlucky. (Note: The schematic illustration represents $u_1 = 1$ at 45° to the x axis, and $a = 0.25$ and $\tau = 1$ arbitrary units.)

more probable than excitation from the localized states within the mobility gap,^{1,14} E_c is assumed to be equal to the band-gap energy E_g . We will distinguish between lucky and unlucky elastic collisions. After a lucky elastic collision, the velocity of a primary carrier has a positive projection on F , and hence, the carrier gains energy from F after the scattering event. In contrast, after unlucky elastic collisions the projection of a carrier velocity on F is negative. Figure 5 illustrates some particular chain of collisions. It is very unlikely that all events are lucky collisions.⁸ Thus, when building up a lucky carrier trajectory, it is necessary to consider a fraction of unlucky collisions. The probability of acquiring E_c is the product of the probability $P_{el}(k, k_u)$ to have k_u unlucky events in the chain of k elastic scattering events (characterized by λ_{el}) and the probability $P_{ie}(k, m)$ to have m inelastic collisions (characterized by λ_{ie} and E_r) in the same chain. The calculations demonstrate a pronounced maximum of the product $P_{el}(k, k_u)P_{ie}(k, m)$ for particular nonzero k_u and m values.⁸

The resulting IIC includes all possible combinations k_u and m that lead to acquiring E_c in the form⁸

$$\alpha = \sum_{m=0}^{\infty} \sum_{k_{||}=0}^{\infty} \frac{P_{el}(k, k_{||}) P_{ie}(k, m)}{l(k)}, \quad (2)$$

where $l(k)$ is the trajectory length in the field direction, which is necessary to pass in order to acquire the ionization threshold energy E_c . The ballistic Shockley model is a specific case of our LD model for $k_{||}=m=0$.

In the above theoretical description it was assumed that charge carriers undergo elastic and inelastic scattering events not affected by trapping and retrapping into localized states in the band tails of the amorphous semiconductor. The reason for this assumption is the following. It has been shown experimentally that charge-carrier mobility becomes deactivated, i.e., only weakly dependent on temperature at electric fields well below the avalanche threshold. This has been shown for both *a*-Se¹ and *a*-Si:H.¹⁷ Therefore, one can conclude that trapping into band tails does not essentially affect the carrier mobility at electric fields close to the avalanche threshold. The deactivation of the carrier mobility by the electric field can be considered as a precursor to the avalanche phenomenon, although not as the cause of this effect. For instance, electron mobility in *a*-Si:H is deactivated at high fields, while the avalanche phenomenon has not yet been established for *a*-Si:H.

IV. APPLICATION OF THE LUCKY-DRIFT MODEL TO THE CASES OF IMPACT IONIZATION IN *a*-Se AND *a*-Si:H

In order to calculate the production of EHP we need to specify material parameters E_c , E_r , λ_{el} , and λ_{ie} . We start by applying our model to *a*-Se, where impact ionization and avalanche multiplication phenomena have been evidenced in numerous experiments including the present study. The band gap of *a*-Se has been reported to be 2.0–2.3 eV in previous studies, the precise value depending on the type of measurement approach.^{25–28} For the present work we take the case $E_c=2.3$ eV, which is most difficult for the initiation of impact ionization. The phonon energy E_r for *a*-Se is derived from the Raman measurements performed in a separate experiment on the HARP target using a DILOR XY micro-Raman spectrometer, with a 647 nm red light from a He–Ne laser in a backscattering geometry. The Raman spectrum is dominated by a broad peak centered at 250 cm^{-1} , which corresponds to $E_r=31$ meV, in agreement with previously published data.²⁹ λ_{el} and λ_{ie} are considered in our model to be free parameters chosen from the best fit to the observed F dependence of the IIC. For *a*-Se the comparison between measured and calculated IIC(F) is given in Fig. 3. Taking $\lambda_{el}=6$ Å and $\lambda_{ie}=72$ Å leads to a reasonable fit to the experimental IIC(F) with, however, a greater slope of the theoretical curve compared to the experimental data. It is remarkable that the inelastic mean-free path appears larger by an order of magnitude than the elastic one. The similar relationship between λ_{el} and λ_{ie} was assumed in Ref. 30 to explain the carrier mobilities in *a*-Se and *a*-Si:H. The greater slope could be caused by two factors. First, we took E_c to be the highest possible (2.3 eV), whereas E_c can be as low as 2.0 eV and the ionization energy itself can be even lower

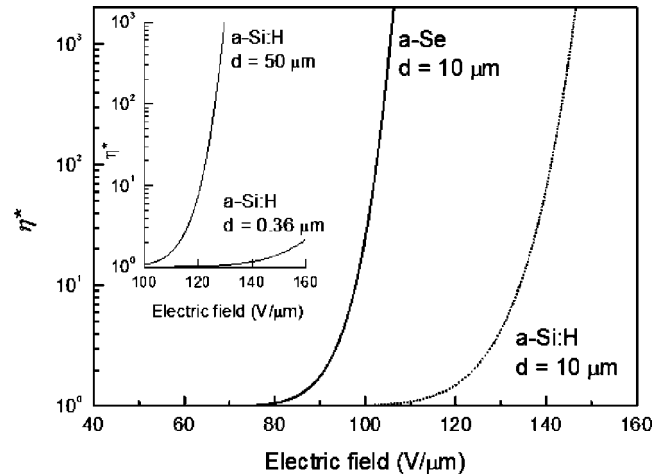


FIG. 6. Field dependence of the multiplication coefficient calculated using Eqs. (1) and (2) for *a*-Si:H ($E_c=1.8$ eV, $E_r=80$ meV, $\lambda_{el}=6$ Å, and $\lambda_{ie}/\lambda_{el}=12$)—dotted line and *a*-Se ($E_c=2.3$ eV, $E_r=31$ meV, $\lambda_{el}=6$ Å, and $\lambda_{ie}/\lambda_{el}=12$)—solid line. The sample thickness d is assumed to be 10 μm . Inset: calculations for *a*-Si:H samples with thicknesses 50 and 0.36 μm .

than the width E_g of the mobility gap. In fact, the impact ionization of secondary carriers might need somewhat less energy than E_g , if these secondary carriers are activated into extended states from localized states within the mobility gap as discussed previously.⁸ Second, we took the relaxation lengths λ_{el} and λ_{ie} independent of F and energy.¹⁴ We, therefore, consider the agreement between the experimental data and theory for *a*-Se in Fig. 3 as satisfactory, not wishing to speculate on the precise magnitudes of the ionization energy and field- and energy-dependent relaxation lengths.

Let us now consider conditions for impact ionization and possible avalanche multiplication in *a*-Si:H. The width of the mobility gap in *a*-Si:H is estimated as $E_g=1.8$ eV.³¹ In *a*-Si the optical phonon density of states has a maximum at about 60 meV, while in *a*-Si:H it is dominated by a stronger peak at ~ 80 meV. The latter is attributed to the hydrogen local vibrational mode.^{32,33} Therefore, we assume $E_r=80$ meV for *a*-Si:H. Taking these estimates for E_c and E_r , and leaving the values of parameters λ_{el} and λ_{ie} equal to those established above for *a*-Se, we can obtain the F dependence of η^* for any *a*-Si:H sample thickness. Figure 6 shows the calculated results for a $d=10$ μm thick *a*-Si:H layer together with the results for the *a*-Se sample of the same d . Remarkably, in *a*-Si:H the change of d from 10 to 50 μm does not affect the predicted threshold field F_{th} significantly (Fig. 6, inset). As it is seen from Fig. 6, the LD model predicts a considerable shift of the threshold field for impact ionization F_{th} in *a*-Si:H with respect to that in *a*-Se. While in *a*-Se $F_{th}\sim 80$ V/ μm , F_{th} in *a*-Si:H is predicted to be above ~ 110 V/ μm , provided λ_{el} and λ_{ie} have the same values in both materials. The difference between F_{th} in *a*-Si:H as compared to *a*-Se is apparently caused by the difference between the phonon energies ($E_r=80$ meV in *a*-Si:H; $E_r=31$ meV in *a*-Se). Due to higher phonon energy in *a*-Si:H, the inelastic scattering processes limit the energy gain from F of the primary charge carriers much more effectively than in *a*-Se. Therefore, higher F is needed to achieve impact ionization in *a*-Si:H even though the necessary ionization energy in

a -Si:H is lower than that in a -Se. Thus, the results of our calculations explain the lack of observations for the impact ionization in a -Si:H at fields up to $100 \text{ V}/\mu\text{m}$.

Avalanche multiplication phenomenon in a -Si:H has been reported by Akiyama *et al.*²⁰ at fields above $150 \text{ V}/\mu\text{m}$ as shown in Fig. 4, although on very thin samples (thickness $0.36 \mu\text{m}$). As it is seen from the inset in Fig. 6 for such a thin a -Si:H sample the theory predicts $\eta^* \sim 2$ for $F \sim 160 \text{ V}/\mu\text{m}$. This is quite different from the measured result presented in Fig. 4, where η^* of 2 corresponds to $\sim 200 \text{ V}/\mu\text{m}$. However, in calculating F in a -Si:H in Fig. 4, the applied voltage was assumed to drop across the i layer (thickness of $0.36 \mu\text{m}$). After applying the correction for voltage drop on the p -type a -SiC:H layer (thickness of $0.14 \mu\text{m}$) the field corresponding to $\eta^* \sim 2$ becomes $140 \text{ V}/\mu\text{m}$. This is quite close to the calculated value of $160 \text{ V}/\mu\text{m}$ for a -Si:H, however, still very large compared with that in a -Se.

V. CONCLUSIONS

We present experimental data on the dependence of the impact ionization coefficient on the electric field obtained on two distinctly different types of a -Se device structures (blocking and insulating) with different thicknesses. Despite the difference between the studied structures, the dependences of the IIC on electric field are similar. The results for a -Se are interpreted using the recently proposed lucky-drift model for amorphous photoconductors (LD).⁸ The comparison between the theoretical and experimental results yields quantitative estimates for the elastic and inelastic relaxation lengths in a -Se. The analysis suggests that scattering processes for holes in a -Se are dominated by elastic scattering events. The agreement between theoretical results and experimental data in a -Se can be achieved assuming that the scattering length of holes due to the disorder potential is about 6 \AA , while the scattering length due to inelastic interaction with phonons is nearly 12 times larger. The energy loss on inelastic phonon scattering of about 31 meV was derived from Raman measurements. Based on the above parameters, the LD model predicts the launch of the avalanche multiplication in a -Se at $80 \text{ V}/\mu\text{m}$ in excellent agreement with the experimental results.

The application of the LD model allows us to answer the intriguing question of why the avalanche multiplication occurs at practical electric fields in a -Se with a wide band gap and rather low carrier mobility, and does not occur at these fields in a -Si:H with a narrower band gap and much higher carrier mobility. The analysis carried out in the frame of the LD model allows us to conclude that the higher phonon energies in a -Si:H as compared to a -Se are responsible for the less efficient gain of energy by the primary charge carriers in the electric field. In fact, the energy gain is impeded by the inelastic scattering processes. As a result, the impact ionization and avalanche multiplication can only be observed in a -Si:H at much higher electric fields (above $160 \text{ V}/\mu\text{m}$) than in a -Se (about $80 \text{ V}/\mu\text{m}$). This agrees with the experimental results obtained so far and does not leave hope that

a -Si:H can compete with a -Se for practical use in avalanche photodetectors.

ACKNOWLEDGMENTS

A.R. is grateful to Professor B. Weinstein (State University of New York at Buffalo) for helpful discussions and for the Raman measurements. O.R. and S.D.B. gratefully acknowledge the financial support of the Deutsche Forschungsgemeinschaft, European Community [IP "FULLSPEC-TRUM" (Ref. N: SES6-CT-2003-502620)], and of the Fonds der Chemischen Industrie. A.R. and J.A.R. gratefully acknowledge the financial support of Canadian Institutes of Health Research (Operating Grant Number 160536) and Cancer Imaging Network of Ontario.

- ¹G. Juska and K. Arlauskas, *Phys. Status Solidi A* **59**, 389 (1980).
- ²M. Kubota, T. Kato, S. Suzuki, H. Maruyama, K. Shidara, K. Tanioka, K. Sameshima, T. Makishima, K. Tsuji, T. Hirai, and T. Yoshida, *IEEE Trans. Broadcast.* **42**, 251 (1996).
- ³K. Tanioka, J. Yamzaki, K. Shidara, K. K. Taketoshi, T. Kawamura, T. Hirai, and Y. Takasaki, in *Advances in Electronics and Electron Physics*, edited by P. W. Hawkes and B. L. Morgan (Academic, London, 1988), Vol. 74, p. 379.
- ⁴T. Watabe, M. Goto, H. Ohtake, H. Maruyama, M. Abe, K. Tanioka, and N. Egami, *IEEE Trans. Electron Devices* **50**, 63 (2003).
- ⁵W. Zhao, D. Li, A. Reznik, B. J. M. Lui, D. C. Hunt, J. A. Rowlands, Y. Ohkawa, and K. Tanioka, *Med. Phys.* **32**, 2954 (2005).
- ⁶A. Reznik, B. J. M. Lui, and J. A. Rowlands, *Technol. Cancer Res. Treat.* **4**, 61 (2005).
- ⁷B. J. M. Lui, D. C. Hunt, A. Reznik, K. Tanioka, and J. A. Rowlands, *Med. Phys.* **33**, 3183 (2006).
- ⁸O. Rubel, S. D. Baranovskii, I. P. Zvyagin, and S. O. Kasap, *Phys. Status Solidi C* **1**, 1186 (2004).
- ⁹B. K. Ridley, *J. Phys. C* **16**, 3373 (1983).
- ¹⁰B. K. Ridley, *J. Phys. C* **16**, 4733 (1983).
- ¹¹M. G. Burt, *J. Phys. C* **18**, L477 (1985).
- ¹²S. McKenzie and M. G. Burt, *J. Phys. C* **19**, 1959 (1986).
- ¹³S. McKenzie and M. G. Burt, *Semicond. Sci. Technol.* **2**, 275 (1987).
- ¹⁴S. O. Kasap, S. D. Baranovskii, K. Tanioka, and J. A. Rowlands, *J. Appl. Phys.* **96**, 2037 (2004).
- ¹⁵D. Adler, M. S. Shur, M. Silver, and S. R. Ovshinsky, *J. Appl. Phys.* **51**, 3289 (1980).
- ¹⁶M. A. Popescu, *Non-Crystalline Chalcogenides* (Kluwer Academic, Dordrecht, The Netherlands, 2000), Chap. 4, p. 293.
- ¹⁷G. Juska, K. Arlauskas, J. Kocka, M. Hoheisel, and P. Chabloz, *Phys. Rev. Lett.* **75**, 2984 (1995) (and references therein).
- ¹⁸W. Futako, T. Sugawara, T. Kamiya, and I. Shimizu, *J. Organomet. Chem.* **611**, 525 (2000).
- ¹⁹B. Chevrier and B. Equer, *J. Appl. Phys.* **76**, 7415 (1994).
- ²⁰M. Akiyama, M. Hanada, H. Takao, K. Sawada, and M. Ishida, *Jpn. J. Appl. Phys., Part 1* **41**, 2552 (2002).
- ²¹J. Allam and J. P. R. David, *Hot Carriers in Semiconductors*, edited by K. Hess, J.-P. Leburton, and U. Ravaioli (Plenum, New York, 1996), p. 343, and references therein.
- ²²A. Cesny, G. Juska, and E. Montrimas, in *Semiconducting Chalcogenide Glass II: Properties of Chalcogenide Glasses*, edited by R. Fairman and B. Ushkov (Elsevier Academic, New York, 2004), p. 15.
- ²³A. Reznik, B. J. M. Lui, Y. Ohkawa, T. Matsubara, K. Miyakawa, M. Kubota, K. Tanioka, T. Kawai, W. Zhao, and J. A. Rowlands, *Nucl. Instrum. Methods Phys. Res. A* **567**, 93 (2006).
- ²⁴G. Juska, J. Kocka, K. Arlauskas, and G. Jukonis, *Solid State Commun.* **75**, 531 (1990).
- ²⁵G. Juska, K. Arlauskas, and E. Montrimas, *J. Non-Cryst. Solids* **97-98**, 559 (1987).
- ²⁶B. Vanhuysse, W. Grevendonk, G. J. Adriaenssens, and J. Dauwen, *Phys. Rev. B* **35**, 9298 (1987).
- ²⁷M. Abkowitz, *Philos. Mag. Lett.* **58**, 53 (1988).
- ²⁸W. C. Tan, G. E. Belev, K. Koughia, R. Johanson, S. O'Leary, and S. Kasap, *J. Mater. Sci. Mater. Electron.* **18**, 429 (2007).
- ²⁹E. Mytilineou and A. Kolobov, in *Amorphous Semiconductors*, edited by

A. V. Kolobov (Wiley, New York, 2003), p. 54.

³⁰G. Juska and K. Arlauskas, *Solid State Phenom.* **44-46**, 551 (1995).

³¹J. Singh and K. Shimakawa, *Advances in Amorphous Semiconductors* (Routledge, Taylor and Francis, London, 2003).

³²W. A. Kamitakahara, H. R. Shanks, J. F. McClelland, U. Buchenau, F. Gompf, and L. Pintschovius, *Phys. Rev. Lett.* **52**, 644 (1984).

³³A. A. Langford, M. L. Fleet, B. P. Nelson, W. A. Lanford, and N. Maley, *Phys. Rev. B* **45**, 13367 (1992).